Design of Test Benches for the Hovering Performance of Nano-Rotors

Zhen Liu[1, †*], Jean-Marc Moschetta[2, †], Nathan Chapman[3, ‡], Roger Barènes[4, †]
[†]*Institut Supérieur de l'Aéronautique et de l'Espace*, University of Toulouse, Toulouse 31400, France
[*]*North-Western Polytechnical University*, Xi'an 710072, China
[‡]*University of Bath*, Bath, BA2 7AY, UK

ABSTRACT

With the reduction of rotor diameter and motor size, the hovering performance measurement becomes a challenge for rotary wing NAVs. Five test benches with highly sensitive mechanism systems have been successively designed in view of being able to measure the thrust and torque of nano-rotors simultaneously and response to the change of variables rapidly with sufficient accuracy. A commercial micro brushless motor and a micro rotor have been studied experimentally and computationally. Computational and experimental comparisons have been carried out and the performance of the test benches has been discussed. The analysis suggests that the thrust coefficients measured by each test bench vary a little from each other, while the power coefficients present significant differences. Then the hovering performance of the micro rotor and power efficiency of the motor were studied. Degradation of motor efficiency and rotor figure of merit are observed with size reduction associated with Nano Air Vehicle applications.

1 INTRODUCTION

Micro Aerial Vehicles (MAVs) have developed quickly since the end of the last century with the emerging requirements of civilian applications, homeland security and military objectives. At present, more complicated battlefield environments or civilian security situations force soldiers to implement MAVs in urban missions. Therefore, an ever-present need has emerged to improve MAV capabilities, enabling the timely collection of comprehensive intelligence information, particularly on the ground in urban terrain. However, current MAVs are too large to provide situational awareness to the users; consequently, even smaller Unmanned Air Vehicles (UAVs) are required to allow reconnaissance inside buildings, penetration of narrow entries and transmission of data without being detected. Therefore, Nano Air Vehicles (NAVs) were proposed to fulfil such missions. Referring to the definition proposed by DARPA, a NAV is defined as a UAV whose maximum dimension should not exceed 3 inches (7.5 cm) and maximum weight should be less than 10 g [1]. Because of the special requirement of this kind of aerial vehicle, it should be able to autonomously enter buildings, stare, spot targets and transmit data at a fairly low speed or hovering mode. Hence, compared with the conventional MAV, a NAV not only has a smaller size but also the requirement of a low-speed flight and hovering ability. Furthermore, it is expected that NAVs should have an endurance of 20 minutes to complete a recognition mission within a range of less than 1 km. Consequently, the propulsion efficiency becomes a quite important parameter for NAV design. In addition, hovering performance is always a bottleneck for the design of small unmanned air vehicles as a result of the degradation of the aerodynamic performance at low Reynolds numbers. Thus, the hovering performance of NAVs will be investigated in this paper.

Presently, two concepts are largely studied in the design of NAVs. One is the rotary wing; the other is the flapping wing. Previous studies have shown that the rotary-wing concept has almost the same hovering performance as flapping wings with a dimension of 7.5cm and a mass of 10g. As rotary-wing concepts can draw from existing theory as well as the high reliability and efficiency of helicopters, this propulsion method was adopted as the preferred NAV concept at ISAE. In order to study the hovering performance of rotary-wing NAVs, the propulsive efficiency of rotors is an interesting issue. However, as a result of the dimension and weight constrains of NAVs, the rotor diameter and the motor weight are rather small. So with the reduction of the rotor diameter and rotational speed of ultra small motors, measuring both thrust and torque simultaneously with a rapid response poses a challenge. The torque of small rotors – estimated below 0.002N.m – is difficult to measure with a sufficient precision, as is the couple of torque and thrust. Yet, both sets of data are needed to have access to the propulsion set efficiency and the figure of merit (FM) of the rotor.

In recent years, several studies [2] [3] [4] have been reported for small rotors or propellers. However, in most studies, either the test bench was designed for separate measurements of thrust and torque, or the rotational speed and rotor diameter were larger than what is currently necessary for the NAV range. So, a test bench design for nano-rotors of the NAV range was required, which would allow to simultaneously measure torque and thrust. In this study, five benches were successively developed with different sensitive mechanism systems. Calibrations of test benches were performed to eliminate nonlinearity of load cell and uncertainty factors. Experiments were carried out with the same motor and rotor on each bench and

[1] PhD candidate, current address: ISAE 31400 Toulouse, France, E-mail: Zhen.Liu@isae.fr
[2] Professor of Aerodynamics, Department of Aerodynamics, Energetics and Propulsion, E-mail: jean-marc.moschetta@isae.fr
[3] Undergraduate student, University of Bath, UK, nac20@bath.ac.uk
[4] Research Scientist, Department of Aerodynamics, Energetics and Propulsion, roger.barenes@isae.fr

comparisons were made to find out their advantages and disadvantages. The rotor is calculated with low-Re software and results are compared with those of experiments. At last, hovering performance of the rotor and work efficiency of the motor were analyzed.

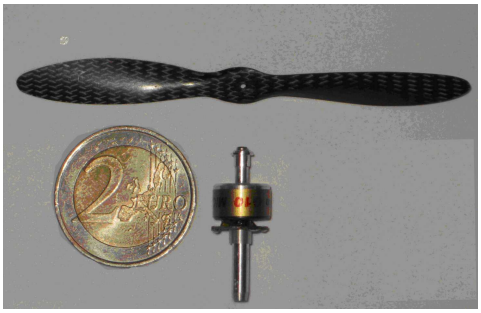

Figure 1: Micro motor and rotor MCF3225

The brushless out-runner motor MICRO and carbon rotor MCF3225 from the company MicroInvent were tested in the experiment as shown in Figure 1. The mass of the motor MICRO is about 2.40g and the maximum thrust is declared to be 24g. MCF3225 is a $81mm \times 63mm$ propeller weighing only 0.2g [5].

2 TEST BENCH DESIGNS AND EXPERIMENTAL METHODOLOGIES

2.1 Rotor performance calculations

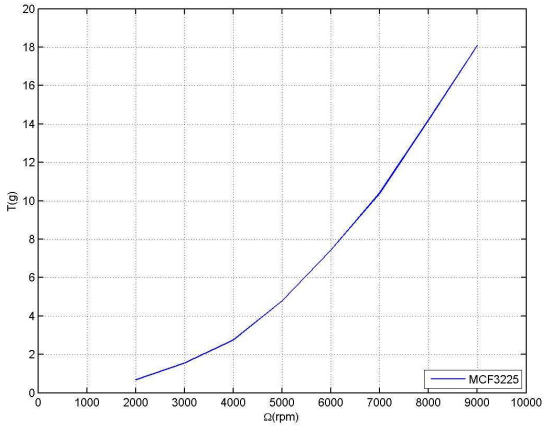

Figure 2: Thrust vs. rotational speed

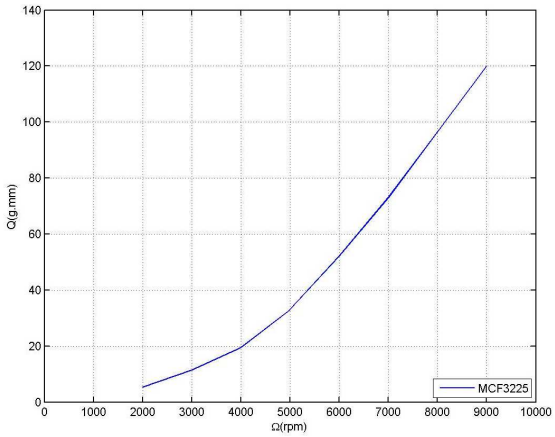

Figure 3: Torque vs. rotational speed

To design a test bench, it is necessary to have a general overview of rotor propulsion performance. Therefore, the thrust and torque of the MCF3225 rotor were estimated as an intial reference to design the test bench. Since the rotor is fabricated for commercial purposes, the distribution of chord, the pitch angle and the airfoil forms are unknown. In addition, the rotor blade is made of very thin carbon, making conventional measurement applications impossible. The chord and twist distributions were determined by *PropellerScanner*[6] with images of the front and side view of the rotor. As the rotor blades are relatively thin, the airfoil could be treated as a curve with thickness and the airfoil form obtained by imprinting a special material with the blade cross-section. With the geometric parameters of the airfoil thus determined, the aerodynamic performance could be calculated. The Reynolds number at which the rotor functions is usually lower than 20,000 so that the laminar separation bubble (LSB) is always induced, although laminar flow dominates in the boundary layer. Most computational fluid dynamics software packages have no ability to simulate transitional flow, whereas XFOIL[7] has been found to be capable of capturing the LSB at a low Re. Therefore, this 2-D airfoil analysis packageI was used to compute the airfoil's aerodynamic performance data, calculated at several ultra-low Reynolds numbers, which would be achieved by altering the rotor's rotational speed. XROTOR [7], a package for analyzing and optimizing a full-scale 3-D propeller, was subsequently used with the rotor's geometric information, the airfoil's aerodynamic parameters, and a very small forward flight speed to compute the rotor's performance characteristics. The potential solution of Goldstein is utilized in the calculation, which is able to take tip boundary conditions and a finite hub into account. The rotational speed was increased from 1,000 RPM to 9,000 RPM. Figure 2 and Figure 3 present the thrust and torque variation with rotational speed, which increase sharply with increasing rotational speeds; ultimately a thrust of only about 18g and a torque of about 120g.mm can be achieved at 9,000 RPM. Such small values will augment the difficulty of obtaining accurate measurements, and as a consequence precise load cells will be chosen in the test bench design, along with a mechanism to amplify thrust and torque outputs.

2.2 Test bench 1

At the first stage, test bench 1 was designed as shown in the Figure 4. It is composed of five parts: an energy supply system, thrust and torque measurement system, speed measurement system, electric parameter measurement system and control and data acquisition system. The energy supply system is a regulated DC power supply which can adjust the voltage and stabilize it at a certain value to ensure the same input. The thrust and torque measurement system includes a mechanism to separate the thrust and torque load cells from each other. Two beam load cells MEIRI F1200, sized at a capacity of 0.5N from calculated estimates, were used to measure thrust and torque. Te small mass of the motor and rotor allowed the load cells to be used as supporting beams, as shown in Figure 4. However, the main obstacle of the design was the separation of thrust and torque to allow them to be measured independently. A mechanism, shown in Figure 4 (b), was developed to

transform the movement of rotation induced by torque to a linear movement orthogonal to the direction of thrust; this mechanism was also desirable as it amplified the torque measured. As shown in Figure 5, the cube rotated with the adjoined pieces when the rotor applied a torque, pushing the bearing connected with the load cell and generating a force F2. At the same time, the bearing applied force F1 on the cube, opposite to F2; L1 was the lever arm of F1and L2 the lever arm of F2. If the torque generated by the rotor was M1 and torque imposed on the load cell was M2, then the equation is given as follows,

$$M2/M1 = (F2 \times L2)/(F1 \times L1) = L2/L1. \quad (1)$$

Hereby, the rotor torque was transferred to the load cell with an amplification of L2/L1. The speed measurement system was made up of a laser emitter and a detector by which the rotational speed could be measured and then transferred to an USB analog-to-digital data acquisition (DAQ); we used NI USB-6229 BNC by National Instruments. The electric parameter measurement system consists of an amperometer and voltmeter to measure the current and voltage passing through the controller. The control and data acquisition system includes the controller, DAQ instrument, computer and processing software. The controller was a YGE4-BL from the Wes-Technik company for brushless motors. During tests, the DAQ worked in both directions: a command generated by the computer software was transmitted to the speed controller via this device, and the measurements acquired during the experiment (voltage, current, thrust, torque and rotational speed) were relayed back to the software as well.

During the experiment, the beam load cell deformed when a force acted on it, which was converted to an altering voltage and recorded by the DAQ. In general, load cells are adjusted at two points by adding the known mass or torque to obtain the linear relationship between the deformation and voltage at the beginning of experiments. Load cells are treated as behaving linearly with the force imposed on them. In fact, the small magnitude of torque and thrust meant the nonlinearity of the load cell and deformation or other unknown factors could affect measurements. Therefore, detailed test bench calibrations were carried out before experiments to improve the precision of results. Since the thrust and torque are fairly small, the units of gram and g·mm were used. Calibrations of thrust and torque are shown in Figure 6 and Figure 7 respectively. In figures, the thrust added and torque added are the known mass or torque added on the test bench, while thrust measured and torque measured are quantities measured by the test bench. Two one-order polynomial functions (straight lines) were fitted respectively so that a relationship between the measured value and real value could be established. However, fitted functions will introduce errors into the results. If the relative fit error is defined as the ratio of the difference between the real value added on test bench and the fitted value obtained from the function to the real value, then the relative fit error for thrust is below 3% when the thrust is great than 2g, and for torque it is below 7% when the torque is above 15 g·mm. In general, the working range of the thrust and torque is beyond 2g and 15 g·mm respectively for NAVs. Therefore, fitted functions are appropriate to give a reasonable precision for results.

After the calibration, adjustments were done to balance the blade before experiments since most rotors may not have a symmetric mass for both blades due to fabrication errors. Then the motor and rotor were installed on the test bench for measurement and the preparation of experiments was ready. At a certain voltage, the rotational velocity could be adjusted by the controller with signals from the data acquisition software. To increase the precision of results, measurements were repeated multiple times. As a verification of the test benches, only results of a brushless out-runner motor MICRO and a rotor of MCF3225 are posted in the following part.

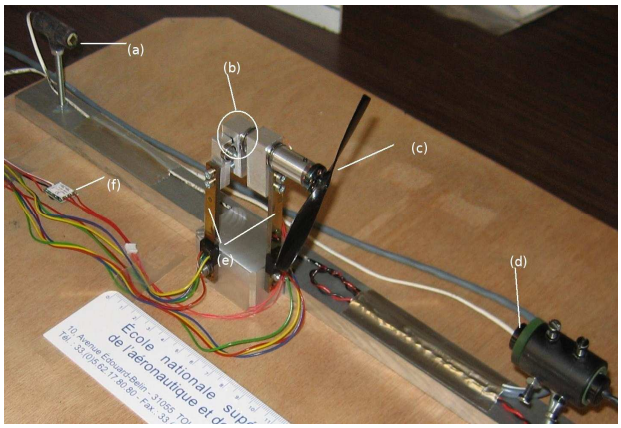

Figure 4: Test bench 1 (a)Laser detector (b)Torque transformation system (c)Motor and rotor (d) Laser emitter (e)Beam load cell (f) controller

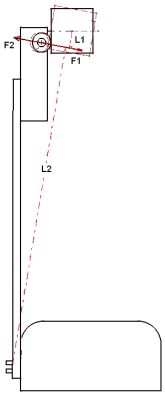

Figure 5: Principle of the torque measurement

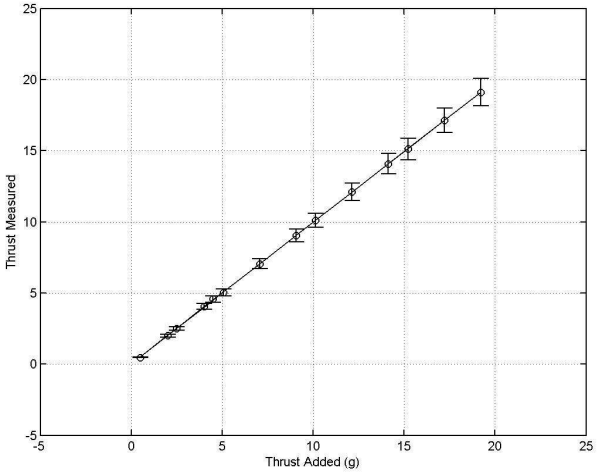

Figure 6: Thrust calibration of test bench 1

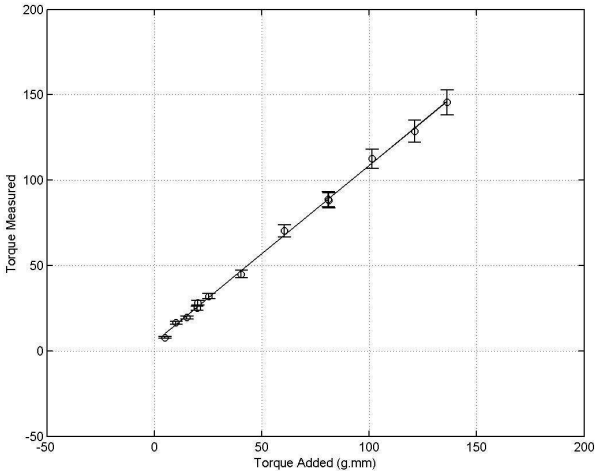

Figure 7: Torque calibration of test bench 1

2.3 Test Bench 2 - Micro Bench

As shown in Figure 4, the test bench 1 is mainly composed of two load cells, which confine its beam length and height of rotor axis; as a result, the mechanism system and the ground disturb the downstream behind the rotor or the flow around the rotor. Therefore, a new test bench was desired. After analyzing the faults of test bench 1, a micro bench, originally was used for bigger motors and propellers in wind tunnel tests, was utilised to measure the motor MICRO and rotor MCF3225 in the configuration shown in Figure 8.

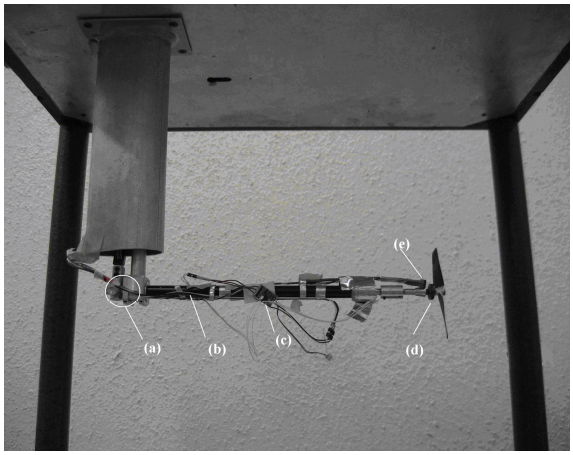

Figure 8: Micro bench (a) Torque transformation system (b) Supporting beam (c) Controller (d) Motor and rotor (e) Velocity measurement instrument

Compared with test bench 1, the micro bench's rotor precedes the supporting frame, thereby reducing the influence of the ground and the mechanism system, which are down stream. The micro bench systems are also similar to those of test bench 1 except that the instrument to measure the rotational velocity and the mechanism system to separate the thrust and torque have been changed, as shown in Figure 8 (e) and (a). With the same principle of test bench 1, the central axis of the horizontal supporting beam rotates with the torque, and then the load cell fixed on the axis will press a bearing hidden in the vertical beam and measure the torque. The measurement of thrust can be acquired by virtue of a four degree-of-freedom system located at the top of the plane, whereas lateral movement is fixed in this experiment. For the micro bench, the thrust will be amplified because of the mechanism, but the torque will not. So in this experiment, the load cell F1200 with a capacity of 2N has been changed to measure the thrust. And because the micro bench is firstly designed as a whole system, the electric system was kept different from test bench 1.

As mentioned above, calibrations are necessary before carrying out the experiments. So the micro bench was calibrated at first as shown in Figure 9 and Figure 10. The results of calibration were fitted by two straight lines, and relative fit errors of both thrust and torque are smaller than that of test bench 1 according to the figures. Relative fit errors of thrust are below 2% when the thrust is greater than 1g, while relative fit errors of torque are below 5% when the toque is greater than 40g.mm. Similarity, the brushless motor MICRO and rotor MCF3225 were tested on the micro bench and the results are stated in the following part.

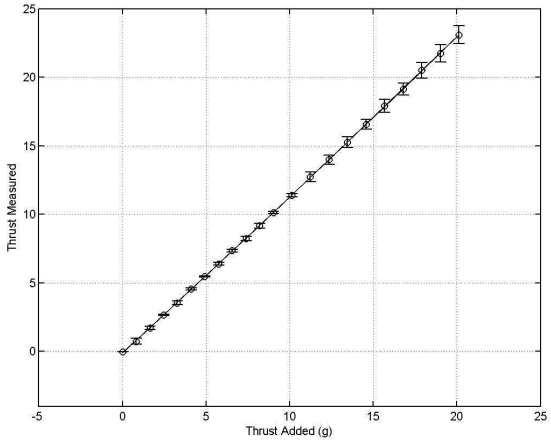

Figure 9: Thrust calibration of micro test bench

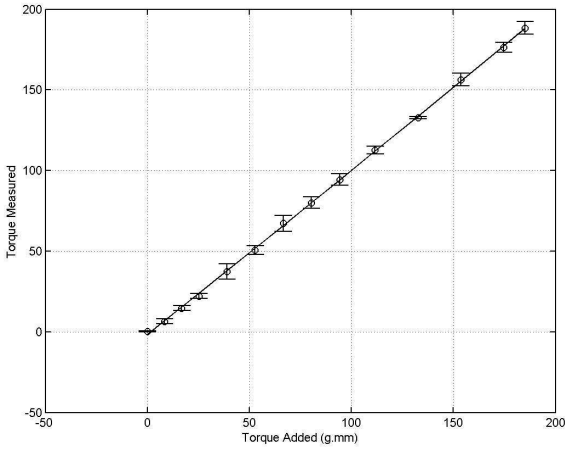

Figure 10: Torque calibration of micro test bench

2.4 Test bench 3 - Nano Bench version 1

Since the micro bench was firstly designed for motors and propellers which have higher thrust and torque than those of NAVs, it failed to measure the torque with acceptable precision. It is assumed that the friction in the micro bench mechanism brought about the increased measurement error. So a new test bench was developed to maintain the micro bench's merit but overcome the friction in the mechanism. Based on this requirement, nano bench version 1 was designed with a highly sensitive mechanism. It was made up

of the same systems as test bench 1, except the thrust and torque measurement system. To implement the separate measurement of coupled thrust and torque, two sharp wedges were orthogonally placed in grooves located on different surfaces, allowing the mechanism to respond simultaneouslyand rapidly to the small changes of the measurement variables. Nano bench version 1 also contains the simplicity of test bench 1 and the long supporting beam high above the ground, as demonstrated on the micro bench.

As shown in Figure 12, the upper wedge with the corresponding groove can only rotate in one direction so that it can only transfer the thrust to the thrust sensor. The lower wedge with the corresponding groove can only rotate in a direction perpendicular to the thrust and transfer the force induced by the torque to the torque sensor. Because these two wedges are orthogonal, the thrust and the torque will not influence each other. With this mechanism, an amplification of about 6 times could be generated for thrust, while no amplification was achieved for torque. Two thin soft metal lines are used to connect the mechanism and load cells to avoid the generation of friction by the contact between the load cell and mechanism. In addition, the load cell for measuring the thrust was changed to a beam load cell MEIRI F1200 with a capacity of 2N.

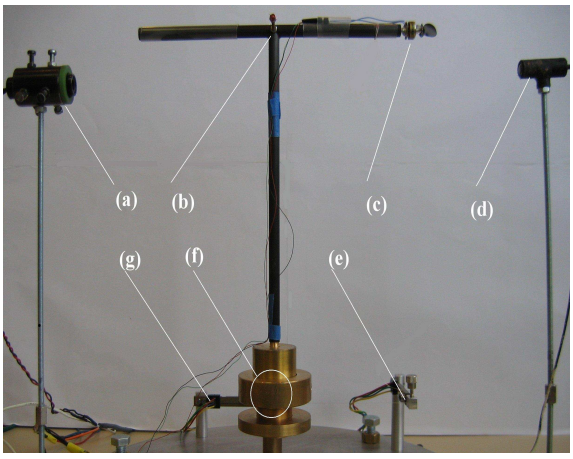

Figure 11: Nano bench version 1 (a) Laser emitter (b) Supporting beams (c) Motor and rotor (d) Laser detector (e)Beam load cell for thrust (f) Mechanism system (g) Beam load cell for torque

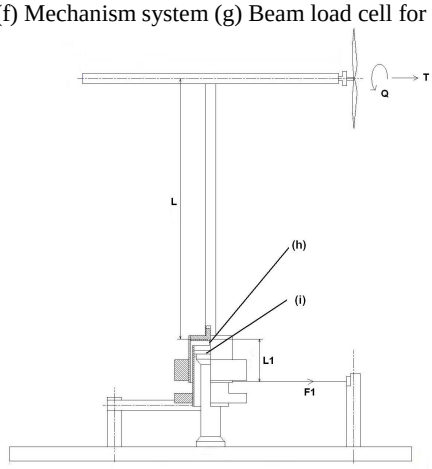

Figure 12: Section view of nano bench version 1
(h) Upper wedge (i) Lower wedge

Due to the nonlinearity of the load cell and the movement of the mechanism, two 2-order polynomial functions were fitted for calibration results. Results are shown in the following figures. Figure 13 and Figure 14 show the calibration results of thrust and toque and corresponding fitted lines. Relative fit errors of thrust are below 0.5% when the thrust is above 1g, while relative fitted errors of torque are below 3% when the toque is above 30g.mm according to analysis. Compared with the other two test benches, nano bench version 1 has higher calibration precision. Motor MICRO and rotor MCF3225 were tested and the results are listed in the following part.

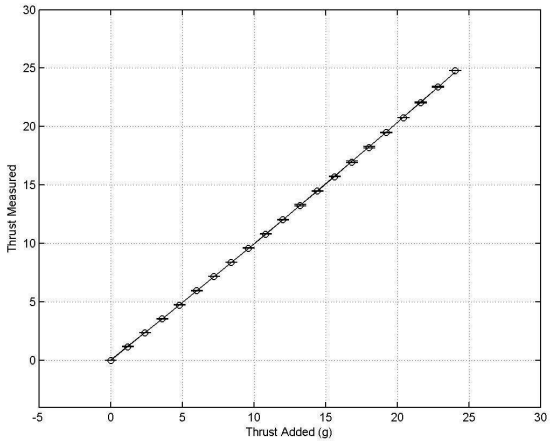

Figure 13: Thrust calibration of nano bench version 1

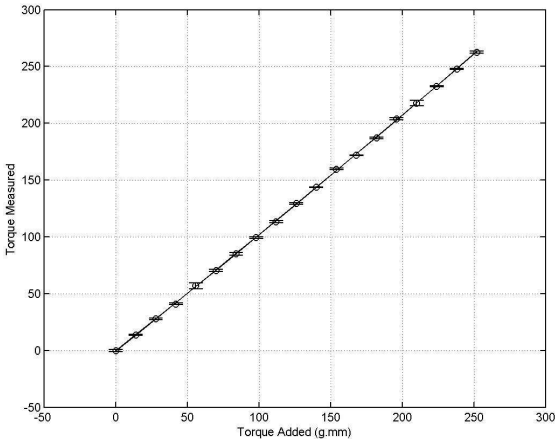

Figure 14: Torque calibration of nano bench version 1

2.5 Test bench 4 - Nano Bench version 2

Despite the fact that Nano bench version 1 shows a high sensitivity and a rapid response to the thrust and torque, some problems have emerged. Very thin and soft wires were utilized along the vertical carbon tube outside of the test bench in order to not generate a force limiting the rotation of the mechanism. However, thin wires augment the inner resistance of the electrical system. Therefore, wires with a larger cross section were passed through the center of the carbon tube between the electrical source and speed controller for nano bench version 2 as shown in Figure 15. Thus, the inner resistance could be reduced with little influence on the torque measurement. In this bench, the elasticity of the load cells and metal wires allows the horizontal beam to transfer the applied forces and therefore deflect to give a reading. Two directions of deflection are induced – thrust and torque – of which the deflection in the thrust direction is larger due to amplification on the bench and that in the direction of the torque is fairly small by virtue of the small magnitude of torque. Although the deflection induced by thrust could be eliminated by the

calibration and the deflection induced by torque is small, the experiment must ensure the attitude of the horizontal beam was constant. Therefore, the length of the vertical beam was shortened to reduce the amplification of the thrust and two micrometer screws were introduced to adjust the attitude of the mechanism during experiments, as shown in Figure 15.

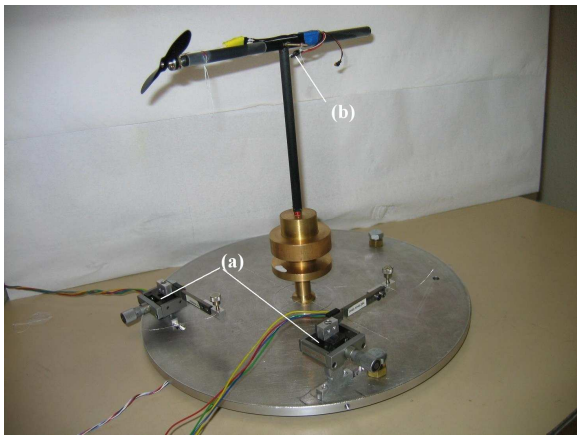

Figure 15: Nano bench version 2 (a) Micrometer screws (b) Wires passing through the carbon tube

Since nano bench version 1 relies on a fairly sensitive mechanism established on the orthogonality of two wedges to separate the coupled thrust and torque, the fabrication of the test bench requires high precision to prevent the interaction of the two variables. The fabrication error of the two wedges as well as potential deviation between the direction of thrust and the axis of the horizontal beam will have an effect on the measurement, especially on the torque. So a calibration allowing for the interaction of the thrust and torque was performed before the experiments. Figure 16 shows that relative fit errors of thrust are below 0.5% when the thrust is above 1g. However, it is observed that the thrust has a strong influence over the torque as shown in Figure 17. For instance, a thrust of about 23 g will produce an extra torque of about -50g.mm. For the torque calibration, on the other hand, relative fit errors are below 8% when the torque is greater than 50g.mm and the influence of torque to thrust is less than -0.1g, even when the torque exceeds 300g.mm. Consequently, the interaction between thrust and torque cannot be neglected, especially for the influence of thrust to torque. For this reason, the experimental results will take this interaction into account before performing calculations. Motor MICRO and rotor MCF3225 were tested in this experiment.

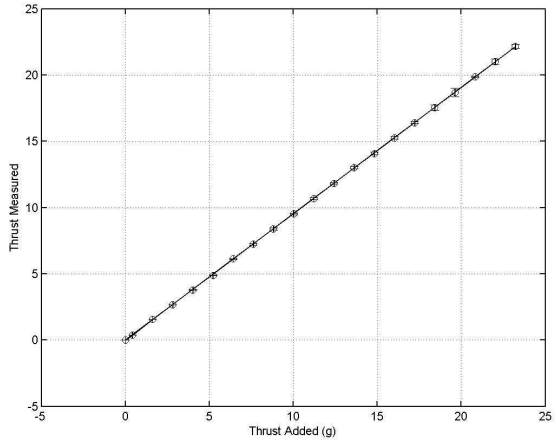

Figure 16: Thrust calibration of nano bench version 2

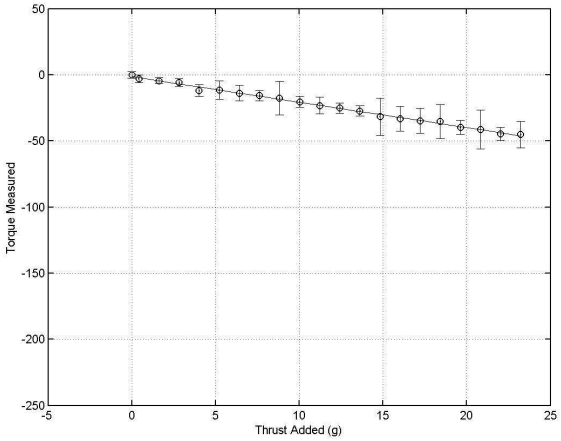

Figure 17: Influence of thrust on torque

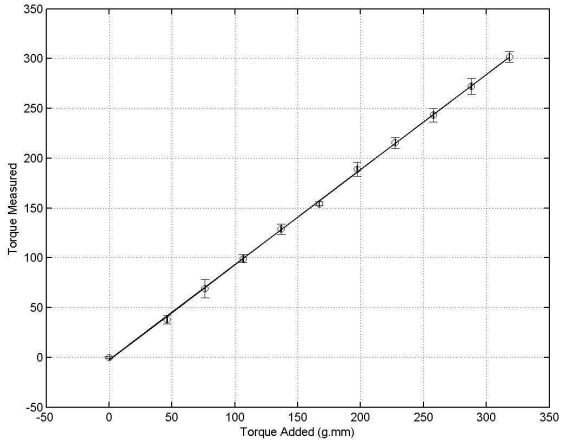

Figure 18: Torque calibration of nano bench version 2

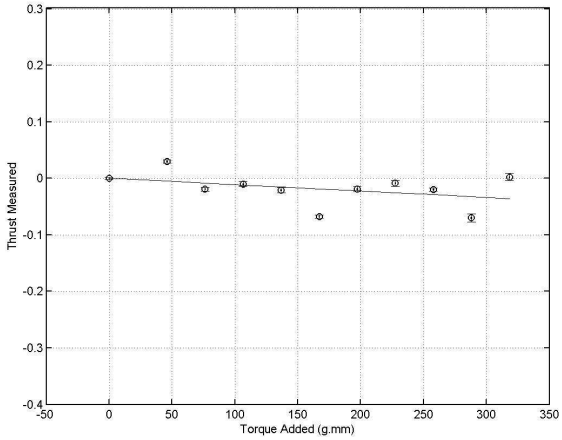

Figure 19: Influence of torque to thrust

2.6 Test bench 6 – Torque Sensor

In the test bench experiments mentioned above, the torque remains a difficulty for measurement. In order to establish the pure torque of the rotor, a static torque sensor DH15 by the SCAIME company with a capacity of 0.005N.mm and an accuracy class of 0.2% was used to measure the torque solely. As shown in Figure 20, the torque sensor has a length of 48 mm and a diameter of 45mm, so an extended supporting beam was installed to avoid the effect of the torque sensor to the rotor downstream. Additionally, short thin wires were adopted to connect the motor to the controller, whose influence on inner resistance were computed during result processing.

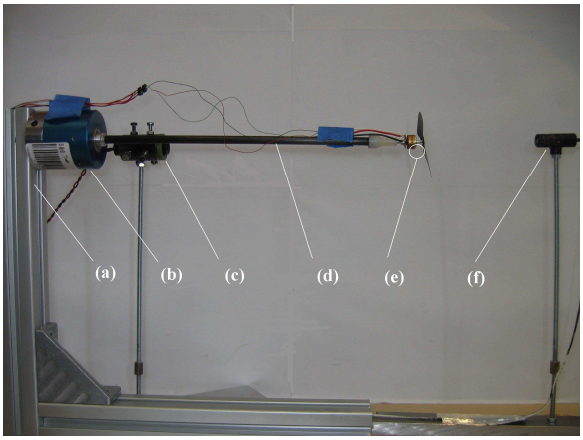

Figure 20: Torque sensor (a)Supporting base (b)Torque sensor (c) Laser emitter (d) Horizontal supporting beam (e) Motor and rotor (f) Laser detector

The calibration was carried out before the experiments as shown in Figure 21. The relative fit errors of torque sensor are below 5% when the torque is above 25 g.mm. Motor micro and rotor MCF3225 were tested with this bench.

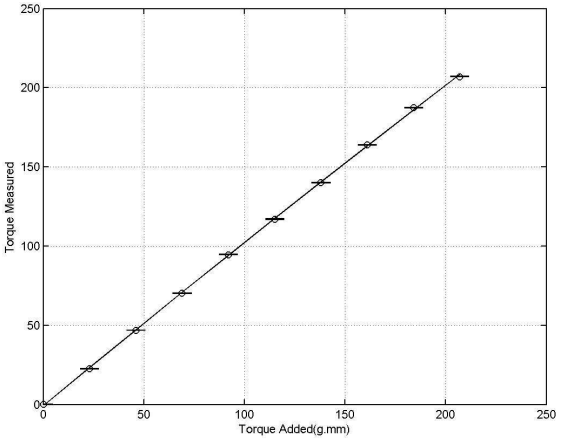

Figure 21: Torque calibration of torque sensor

3 RESULTS AND ANALYSIS

Since the test benches above were developed successively, gradual improvements have been made by introducing numerous modifications to the mechanisms and electric systems. This also brought about distinctions between the results tested by different benches. Comparisons were carried out with the experimental results of the Micro motor and MCF3225 rotor at a voltage of 3.6 V for test bench 1, the micro bench and nano bench version 1 and a voltage of 3.8 V for the nano bench version 2 and torque sensor. All results were presented with error bars of confidence 95%.

As the definitions of propulsive parameters of rotors vary slightly between countries, they are defined before comparing the results. The thrust coefficient C_T and power coefficients C_P are defined as follows,

$$(2) \quad C_T = \frac{T}{\rho A(\Omega R)^2}$$

$$(3) \quad C_P = \frac{P}{\rho A(\Omega R)^3} .$$

For this paper, hovering performance is studied, so the figure of merit (FM) is defined as the ratio of ideal power to the actual power and the motor efficiency η is defined as the ratio of actual power to input electric power,

$$(4) \quad FM = \frac{P_{ideal}}{P} = \frac{C_T^{3/2}}{\sqrt{2}C_P}$$

$$(5) \quad \eta = \frac{P}{UI} = \frac{Q \cdot \Omega}{UI}$$

where T is the thrust; P is the power consumed; Ω is the rotational speed; R is the radius of the blade ; ρ is the density of the air; A is the reference area, usually defined as the disk area; Q is the rotor torque; U is the input voltage and I is the input current.

The solidity σ is defined as,

$$(6) \quad \sigma = \frac{N_b \bar{c}}{\pi R},$$

where N_b is the number of blades and $\bar{c}$ is the average chord length.

Re is defined as the Reynolds number at the 3/4 radius of blade.

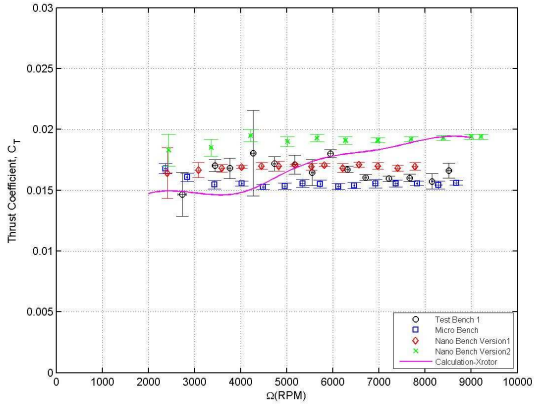

Figure 22: Thrust coefficient at different rotational speeds

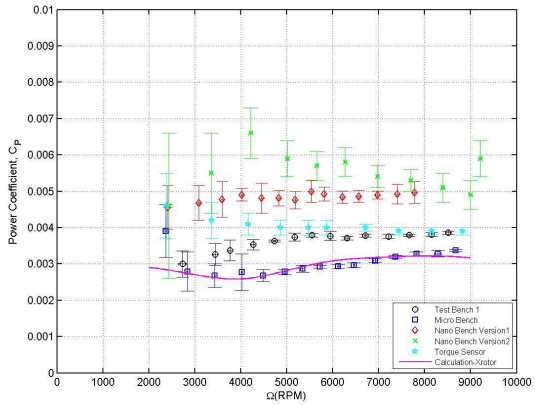

Figure 23: Power coefficient at different rotational speeds

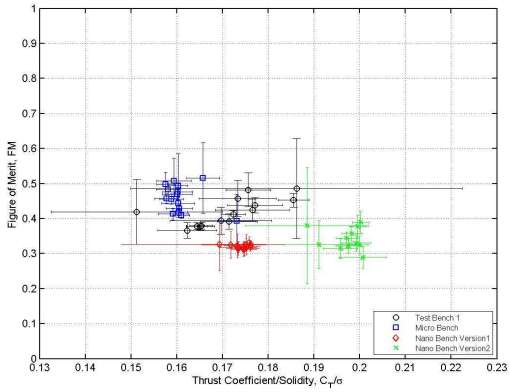

Figure 24: FM vs. ratio of thrust coefficient to rotor solidity

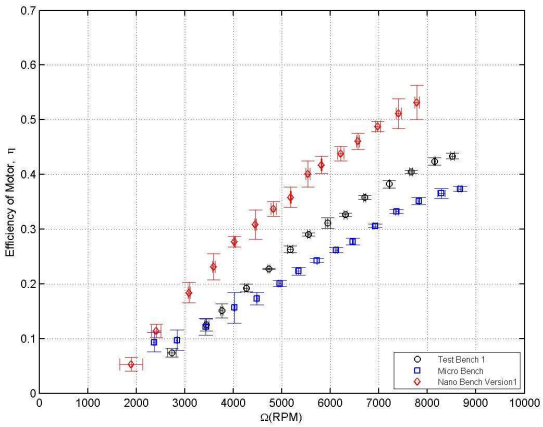

Figure 25: Motor efficiency at different rotational speeds

Figure 22 presents the thrust coefficients at different rotational speeds for all test benches except the torque sensor. The thrust coefficients determined by test bench 1 were not regular, however; they match well with the results on nano bench version 1 at rotational speeds from 3,000 RPM to 6,000 RPM, whereas they approach the results on the micro bench at rotational speeds from 6,500 RPM to 8,000 RPM. Nevertheless, the results for the three test benches vary slightly from each other. However, the nano test bench version 2 tested a higher thrust coefficient than the other test benches, and differences of about 15% could be found between this and version 1. Numerical calculations predict a lower thrust coefficient at rotational speeds less than 4,000 RPM, but match well with nano bench version 2 at rotational speeds above 6,000 RPM. In general, the thrust coefficients lie between 0.015 and 0.02 and the discriminations among the results tested by all the test benches are less than 25% if the average value of thrust coefficient is used as a reference.

Torque measurement is a difficulty for small rotors, especially when the micro rotor rotates at such low speeds. Deters[3] overcame this issue by measuring rotors at very high speeds. Even with great attention to the sensitivity of test benches, the five test benches measured the power coefficients with enormous distinctions. In Figure 23, the test results of power coefficients were presented at different rotational speeds. At low speeds, the power coefficients tested by the torque sensor approach those tested by the nano bench, and the discriminations augment with higher rotational speeds. However, results match well with those of test bench 1, especially when the rotational speed exceeds 5,000 RPM. Nano bench version 2 measured higher power coefficients than the other test benches, and its results approximate those of nano test bench version 1. The micro bench tested the lowest values, but its results match well with computational results from XROTOR.

In this experiment, the Re varies from 4,000 to 20,000. In general, the aerodynamic performance of rotor deteriorates with the reduction of Re. However, the thrust coefficients and power coefficients change slightly with Re and vary from test benches. As shown in Figure 22 and 23, an alteration of less than 15% for thrust coefficient and 35% for the power coefficients could be found. But the tendency and the magnitude of alteration depend on the test benches. The following reason may result in them: 1) firstly, the geometry of propeller has been optimized by the designer for different rotational speed, so that the lift coefficient and the power coefficient doesn't change a lot with the drop of the Re. 2) secondly, the vibration of test bench has flattened or reversed the change.

Figure 24 shows that the figure of merit varies from the ratio of thrust coefficient to solidity. FM measured by test bench 1 and the micro bench is mainly located between 0.4 and 0.5, while that measured by the nano bench version 1 and version 2 is less than 0.4. Figure 25 shows the motor efficiency varies with rotational speed. Since the results of nano bench version 2 were tested at a different voltage, they are omitted from this figure. Although differences exist between the results tested by the three test benches, the motor efficiency rises sharply with the increase of rotational speed for all. The peak value measured by nano bench version 1 is about 0.53 higher than that measured by test bench 1, which is 0.43, and the micro bench, which is 0.37.

Although, when compared with the other test benches, test bench 1 measured values between those found on other benches, short support beams and friction in the mechanism impacted the measurement precision by allowing vibration in the system at low rotational speeds. The micro test bench tested the lowest values among the test benches by virtue of its complicated mechanism, which will cause more friction than other systems and reduce the measuring sensitivity. Despite the fact that nano bench version 1 uses the same mechanism as version 2, the calibration methods and the measurement methods differ greatly between experiments. Whereas nano test bench version 1 did not allow for this possibility, the deformation of the load cell and metal lines in version 2 caused interaction between the thrust and torque. Even taking this into account, uncertainties such as propeller asymmetry and deviation of the motor from the centreline upon installation could have a large influence on the torque measurement for these two versions due to the long lever arm of the main horizontal beam. The torque sensor is supposed to be able to measure the static torque precisely, but the torque is a dynamic variable because of asymmetry of the rotor and motor. However, the ability for this torque sensor to measure the dynamic variable has not been verified. Calculation has underestimated the thrust coefficient at low rotational speeds but overestimated it at high rotational speeds. Because of the small thickness of rotor blades, conventional methods fail to measure the form of the blade precisely. Hereby, an approximate method was adopted in this study, which might result in deviations of the blade's geometric form. On the other hand, XFOIL has been found to predict a laminar separation in advance at ultra low Reynolds numbers[8], and the prediction of profile drag is always a key difficulty for computational software – particularly when the profile drag dominates, as is the case at ultra-low Reynolds numbers. Consequently, the computational error will accumulate, causing differences between the experimental and computational results.

4 CONCLUSIONS

Five test benches, including a bench based on a torque sensor, were designed for the measurement of hovering performance of micro rotors and motors for NAVs. Sensitive mechanisms were developed so that the torque and

thrust are able to be tested simultaneously and quickly. In order to compare the performance of the test benches, experiments were carried out with the MICRO motor and MCF3225 rotor. Results show that the test benches could measure the thrust with a difference of less than 25%. However, great differences were observed for the torque coefficients tested by each bench. In addition, full-scaled helicopters reach figure of merit values of about 0.7 to 0.8[9], though this value declines sharply with decreasing Re number; the experimental results found here indicated the figure of merit of the micro rotor is between 0.3 and 0.5. Even so, the counter-rotating MAV rotors from Maryland University achieved a FM of about 0.55, while the diameter of the rotors was 2 times that of the MCF3225[10]. These experimental results therefore demonstrate the reduction of FM with the drop of the Reynolds number. At the same time, the motor efficiency increases sharply with rotational speed; in the experiments, the maximum motor efficiency is about 0.53, whereas it is about 0.6 for conventional motors. As the small motors are fabricated with thin wires, the inter resistance increases accordingly, resulting in a higher power consumption. Therefore, motor efficiency decreases with a reduction in size. The rotor was also calculated with XFOIL and XROTOR at different rotational speeds, but the computational results vary greatly from the experimental results, especially for the torque measurements.

In conclusion, the current test benches can measure the thrust to a reasonable precision, but fail to measure the torque, and calculations are not able to predict the hovering performance of a rotor precisely. Furthermore, the experimental results of FM and motor efficiency show that the performance of micro rotors and motors decline with the reduction of size.

In light of this information, further modifications will be implemented in order to increase the measurement stability of nano bench version 2. Accurate calibration will be carried out, and comparisons made between the experimental and theoretical results to verify the performance of the various test benches. Furthermore, the method to acquire geometric rotor profiles will be improved, and suitable computational methods should be developed in future work.

5 ACKNOWLEDGEMENTS

The authors would like to thank China Scholarship Council and the laboratory of DAEP of ISAE for the financial and facilities support, and Mr. R. Chanton, Mr. G. Tessarotto and Mr. S. Gérard for help on the design and fabrication of test benches.

REFERENCES

[1] Pines, D.J., and DARPA/DSO, Nano Air Vehicle Program, *BAA06-06S*.

[2] He, R., and Sato, S., Design of a Single-Motor Nano Aerial Vehicle with a Gearless Torque-Canceling Mechanism, *AIAA paper*, 2008-1417.

[3] Deters, R.W., and Selig, M.S., Static Testing of Micro Propellers, *AIAA paper*, 2008-6246.

[4] Schafroth, D., Bouabdallah, S., Bermes, C., and Siegwart, R., From the Test Benches to the First Prototype of the muFly Micro Helicopter, *Spinger Science and Business Mesia B.V.*, s10846-008-9264-z, 2008.

[5] Micro Invent, "MCF3225", http://www.microinvent.com/

[6] Hepperle, M., PropellerScanner Manual, *www. mh-aerotools.de*, 2003.

[7] Drela, M., XFOIL, Xrotor, Softwares, Massachusetts Institute of Technology

[8] Youngren, H., Kroninger, C., Chang, M., and Jameson, S., "Low Reynolds Number Testing of the AG38 Airfoil for the SAMARAI Nano Air Vehicle", AIAA paper, 2008-417.

[9] Leishman, J. G., Principles of Helicopter Aerodynamics, *CambridgeUniv. Press*, New York, 2000, Chap. 5.

[10] Pines, D.J., and Bohorquez, F., "Challenges Facing Future Micro-Air-Vehicle Development", *Journal of Aircraft*, Vol.43, No.2, March-April 2006, pp.290-304.